

# Thermodynamics of lattice QCD with 3 flavours of colour-sextet quarks.

J. B. Kogut

*Department of Energy, Division of High Energy Physics, Washington, DC 20585, USA*  
*and*

*Dept. of Physics – TQHN, Univ. of Maryland,*  
*82 Regents Dr., College Park, MD 20742, USA*

D. K. Sinclair

*HEP Division, Argonne National Laboratory,*  
*9700 South Cass Avenue, Argonne, IL 60439, USA*

We have been studying QCD with 2 flavours of colour-sextet quarks to distinguish whether it is QCD-like or conformal. For comparison we are now studying QCD with 3 flavours of colour-sextet quarks, which is believed to be conformal in the chiral limit. Here we present the results of simulations of lattice QCD with 3 colour-sextet quarks at finite temperatures on lattices of temporal extent  $N_t = 4$  and 6, with masses small enough to yield access to the chiral limit. As for the 2-flavour case, we find well-separated deconfinement and chiral-symmetry restoration transitions, both of which move to appreciably weaker couplings as  $N_t$  is increased from 4 to 6. If this theory is conformal, we would expect there to be a bulk chiral transition at a fixed coupling. For this reason we conclude that for  $N_t = 4$  and 6, the chiral and hence the deconfinement transitions are in the strong-coupling domain where the theory is essentially quenched. The similarity between the behaviours of the 2 and 3 flavour theories suggested that the  $N_t = 4$  and 6 transitions for the 2-flavour theory also lie in the strong-coupling domain. The phase structure of both theories is very similar.

## I. INTRODUCTION

With the LHC starting to probe the Higgs sector of the standard model, studies of models of this sector are timely. We are particularly interested in extensions of the standard model with strongly-coupled (composite) Higgs sectors. The most promising of these are Technicolor theories, QCD-like gauge theories with massless fermions, whose pion-like excitations play the role of the Higgs field, giving masses to the  $W$  and  $Z$  [1, 2]. It has been pointed out that phenomenological difficulties which plague Technicolor theories and their extensions can largely be avoided if the fermion content is such that the running coupling constant evolves very slowly (“walks”) over a considerable range of renormalization scales. Such non-perturbative behaviour is best studied by lattice gauge theory simulations. [3–6]

The most promising candidates for gauge theories which “walk”, are those where the one-loop contribution to the Callan-Symanzik  $\beta$  function implies asymptotic freedom, while the two-loop contribution has the opposite sign. If these two terms describe the physics, the  $\beta$  function has a second zero at non-zero coupling. Such a zero would be an infrared (IR) fixed point for massless quarks, implying that the theory is conformal. However, if a chiral condensate forms before the would-be IR fixed point is reached, the running coupling starts to increase again and the fixed point is avoided. The theory is then QCD-like, but the presence of a nearby fixed point means that there is a region where the coupling constant evolves very slowly and the theory walks.

We have been studying QCD with colour-sextet quarks. If the number of flavours  $N_f = 2$  or 3, the theory is asymptotically free and the two-loop term in the  $\beta$  function has the opposite sign from the one-loop term.  $N_f = 2$  is a candidate walking theory, provided that it is QCD-like. Phenomenological studies such as those of [7, 8] and the references these contain, indicate that further investigations of this 2-flavour theory as a model of walking technicolor, are warranted. Since asymptotic freedom is lost at  $N_f = 3\frac{3}{10}$ , two-loop perturbation theory predicts that  $N_f = 3$  has an IR fixed point at a small enough value of the coupling constant that one might trust perturbation theory. For this reason it is believed that the  $N_f = 3$  theory probably has an IR fixed point, and is thus a conformal field theory. It is therefore useful to compare the behaviour of the  $N_f = 3$  and  $N_f = 2$  theories to see whether they show qualitative differences. We have performed extensive lattice simulations of the  $N_f = 2$  theory at finite temperatures to try and determine whether it is conformal or

QCD-like [9, 10]. These simulations are continuing [11]. Work on the  $N_f = 2$  theory using different actions is being performed by other groups [12–19]. However, a consensus as to whether the theory is conformal or QCD-like has yet to be achieved. In this paper we present simulations of lattice QCD with 3 colour-sextet quarks using the same methods as for the 2-flavour case, for comparison. We simulate lattice QCD with 3 flavours of staggered colour-sextet quarks at finite temperature on lattices with  $N_t = 4$  and 6, using the deconfinement and chiral-symmetry restoration transitions to study the evolution of the running coupling constant. As in the 2-flavour theory we find widely separated deconfinement and chiral-symmetry restoration temperatures. Both transitions move to appreciably weaker couplings as  $N_t$  is increased from 4 to 6. Except that the  $N_f = 3$  transitions are, as expected, at stronger couplings than their  $N_f = 2$  counterparts, the two theories behave very similarly. Since we believe the  $N_f = 3$  theory to be conformal, the weak coupling conformal domain should be separated from the chirally broken region by a bulk chiral transition. Thus the coupling at the chiral transition should be fixed. This strongly suggests that the  $N_t = 4$  and 6 transitions are in the strong-coupling domain where the fermions are bound into a chiral condensate at distances of order the lattice spacing or less, so that the theory is controlled by quenched dynamics. The evolution of the couplings at the transitions between  $N_t = 4$  and 6 occurs because these are finite-temperature transitions of the effectively-quenched theory. It was this observation that suggested to us that the  $N_t = 4$  and 6 transitions of the  $N_f = 2$  theory might also be in the strong-coupling domain. This was born out when we determined the position of its  $N_t = 8$  chiral transition [10].

The  $N_f = 3$  theory shows a clear 3-state signal in the phase of the Wilson Line (Polyakov Loop) just above the deconfinement transition. At even larger values of  $\beta = 6/g^2$ , the 2 states with complex Wilson Lines disorder into a state with a negative Wilson line. This phase structure is very similar to that observed for the  $N_f = 2$  theory.

In section 2 we define our lattice action and discuss our simulation methods. Section 3 describes our simulations and results for  $N_t = 4$ , while section 4 is devoted to our  $N_t = 6$  simulations. We present our discussion and conclusions in section 5.

## II. METHODOLOGY

This section gives a description of our action and simulation methods given in an almost identical form in our earlier publications [9, 10].

For the gauge fields we use the standard Wilson (plaquette) action:

$$S_g = \beta \sum_{\square} \left[ 1 - \frac{1}{3} \text{Re}(\text{Tr}UUUU) \right]. \quad (1)$$

For the fermions we use the unimproved staggered-quark action:

$$S_f = \sum_{\text{sites}} \left[ \sum_{f=1}^{N_f/4} \psi_f^\dagger [\mathcal{D} + m] \psi_f \right], \quad (2)$$

where  $\mathcal{D} = \sum_{\mu} \eta_{\mu} D_{\mu}$  with

$$D_{\mu} \psi(x) = \frac{1}{2} [U_{\mu}^{(6)}(x) \psi(x + \hat{\mu}) - U_{\mu}^{(6)\dagger}(x - \hat{\mu}) \psi(x - \hat{\mu})], \quad (3)$$

where  $U^{(6)}$  is the sextet representation of  $U$ , i.e. the symmetric part of the tensor product  $U \otimes U$ . When  $N_f$  is not a multiple of 4 we use the fermion action:

$$S_f = \sum_{\text{sites}} \chi^\dagger \{ [\mathcal{D} + m] [-\mathcal{D} + m] \}^{N_f/8} \chi. \quad (4)$$

The operator which is raised to a fractional power is positive definite and we choose the real positive root. This yields a well-defined operator. We assume that this defines a sensible field theory in the zero lattice-spacing limit, ignoring the rooting controversy. (See for example [20] for a review and guide to the literature on rooting.)

We use the RHMC method for our simulations [21], where the required powers of the quadratic Dirac operator are replaced by diagonal rational approximations, to the desired precision. By applying a global Metropolis accept/reject step at the end of each trajectory, errors due to the discretization of molecular-dynamics time are removed.

Finite temperature simulations are performed by using a lattice of finite extent  $N_t$  in lattice units in the Euclidean time direction, and of infinite extent  $N_s$  in the spatial direction. In practice this means we choose  $N_s \gg N_t$ . The temperature  $T = 1/N_t a$ , where  $a$  is the lattice spacing. (In our earlier equations we set  $a = 1$ .) Since the deconfinement temperature  $T_d$  and the chiral symmetry restoration temperature  $T_{\chi}$  should not depend on  $a$ , and since  $a = 1/N_t T$ , measuring the coupling  $g$  at  $T_d$  or  $T_{\chi}$  as a function of  $N_t$  gives  $g(a)$  for a series of  $a$  values which approach zero as  $N_t \rightarrow \infty$ . If the ultraviolet behaviour of the theory

is governed by asymptotic freedom,  $g(a)$  should approach zero as  $a \rightarrow 0$ , i.e.  $N_t \rightarrow \infty$ . However, for the 3-flavour theory under consideration in this paper, we expect that the chiral transition is a bulk transition. If so, the coupling at the chiral transition should be a constant, independent of  $N_t$ . (Since the  $\beta$  value at the deconfinement transition ( $\beta_d$ ) is expected to be less than that at the chiral transition ( $\beta_\chi$ ), it follows that  $\beta_d$  will also approach a finite value as  $N_t \rightarrow \infty$ .)

We determine the position of the deconfinement transition as that value of  $\beta$  where the magnitude of the triplet Wilson Line (Polyakov Loop) increases rapidly from a very small value as  $\beta$  increases. The chiral phase transition is at that value of  $\beta$  beyond which the chiral condensate  $\langle \bar{\psi}\psi \rangle$  vanishes in the chiral limit. Because we are forced to simulate at finite quark mass, this value is difficult to determine directly. We therefore estimate the position of the chiral transition by determining the position of the peak in the chiral susceptibility  $\chi_{\bar{\psi}\psi}$  as a function of quark mass, and extrapolating to zero quark mass. The chiral susceptibility is given by

$$\chi_{\bar{\psi}\psi} = V \left[ \langle (\bar{\psi}\psi)^2 \rangle - \langle \bar{\psi}\psi \rangle^2 \right] \quad (5)$$

where the  $\langle \rangle$  indicates an average over the ensemble of gauge configurations and  $V$  is the space-time volume of the lattice. Since the fermion functional integrals have already been performed at this stage, this quantity is actually the disconnected part of the chiral susceptibility. Since we use stochastic estimators for  $\bar{\psi}\psi$ , we obtain an unbiased estimator for this quantity by using several independent estimates for each configuration (5, in fact). Our estimate of  $\langle (\bar{\psi}\psi)^2 \rangle$  is then given by the average of the (10) estimates which are ‘off diagonal’ in the noise.

### III. $N_t = 4$ SIMULATIONS

We simulate lattice QCD with 3 flavours of sextet quarks on  $12^3 \times 4$  lattices starting from an  $N_f = 2$  configuration with a positive Wilson Line (Polyakov Loop) at  $\beta = 6/g^2 = 7.0$ . Three different quark mass values  $m = 0.02$ ,  $m = 0.01$  and  $m = 0.005$  (in lattice units) are used to allow continuation to the chiral limit. For  $m = 0.02$  we choose a set of  $\beta$ s covering the range  $5.0 \leq \beta \leq 7.0$ , for  $m = 0.01$ ,  $5.2 \leq \beta \leq 7.0$ , while for  $m = 0.005$ ,  $5.27 \leq \beta \leq 7.0$ . This covers both the deconfinement and chiral-symmetry restoration transitions. For most values of  $(\beta, m)$  we find 10,000 trajectories to be adequate. We increase this to 50,000

trajectories for values of  $(\beta, m)$  close to the deconfinement transition.

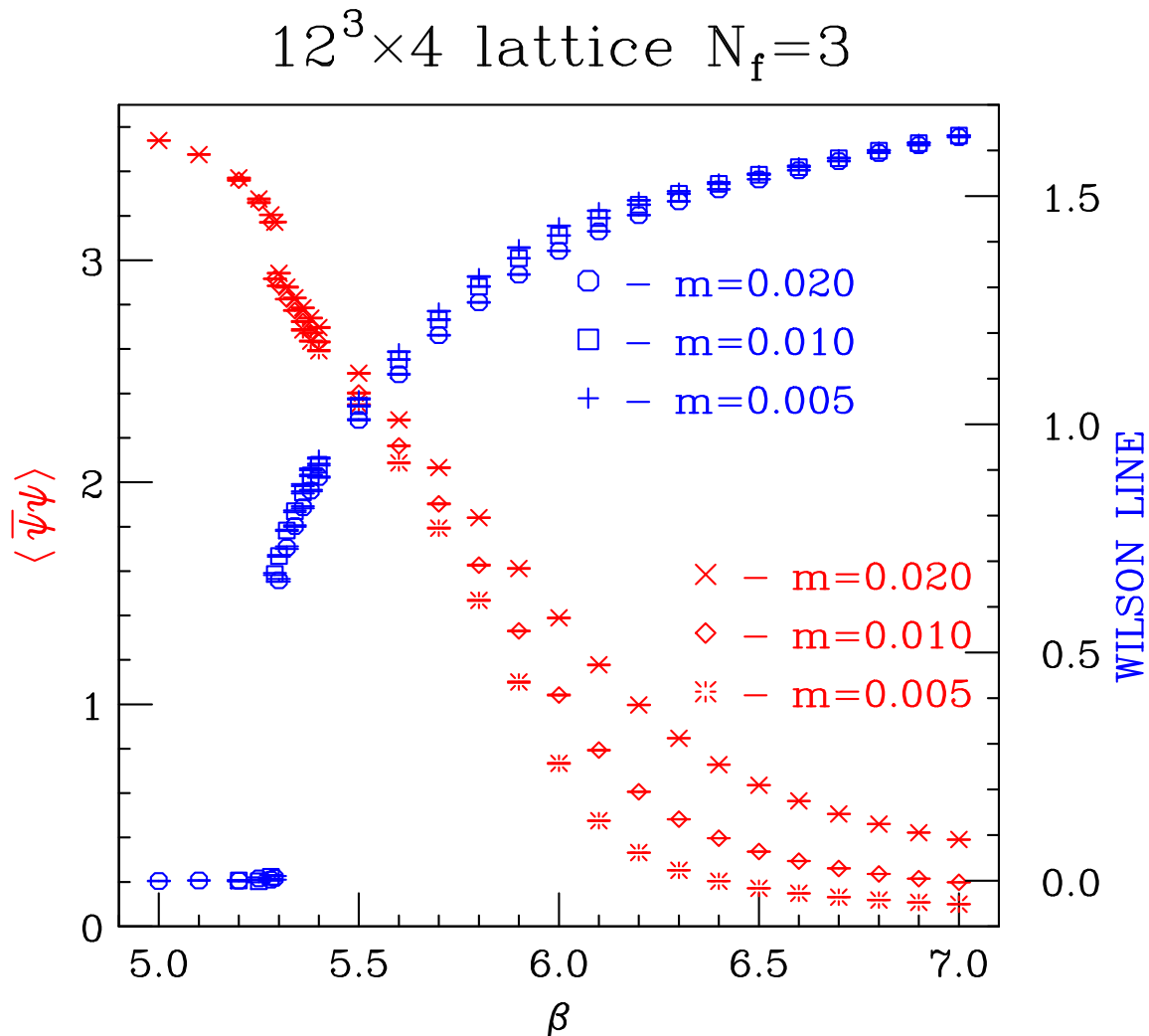


FIG. 1: Wilson Line (Polyakov Loop) and  $\langle \bar{\psi}\psi \rangle$  as functions of  $\beta$  on a  $12^3 \times 4$  lattice.

Figure 1 shows the Wilson Lines and chiral condensates  $\langle \bar{\psi}\psi \rangle$  as functions of  $\beta$  for each of the 3 mass values used in our simulations. The qualitative features of these plots are very clear. At low  $\beta$  values, the Wilson Line is close to zero. At  $\beta \approx 5.3$  or just below, the Wilson Line exhibits a (possibly discontinuous) jump to much larger values. This, we interpret to herald the deconfinement transition. We note, however, that the chiral condensate, while showing a small discontinuity, shows no sign of vanishing even in the chiral limit, at this transition. Hence the deconfinement and chiral transitions are not coincident, in contrast to what happens for fundamental quarks where all the evidence favours chiral-symmetry restoration *at* the deconfinement transition. Pinpointing the chiral transition is

more difficult, since this requires extrapolating the chiral condensate to zero quark mass in the region where it has strong dependence on the quark mass, to find where it vanishes. A cursory examination of the figure would suggest that this occurs somewhere around  $\beta = 6$ . Hence the chiral and deconfinement transitions are far apart with the chiral phase transition occurring at a much weaker coupling than the deconfinement transition.

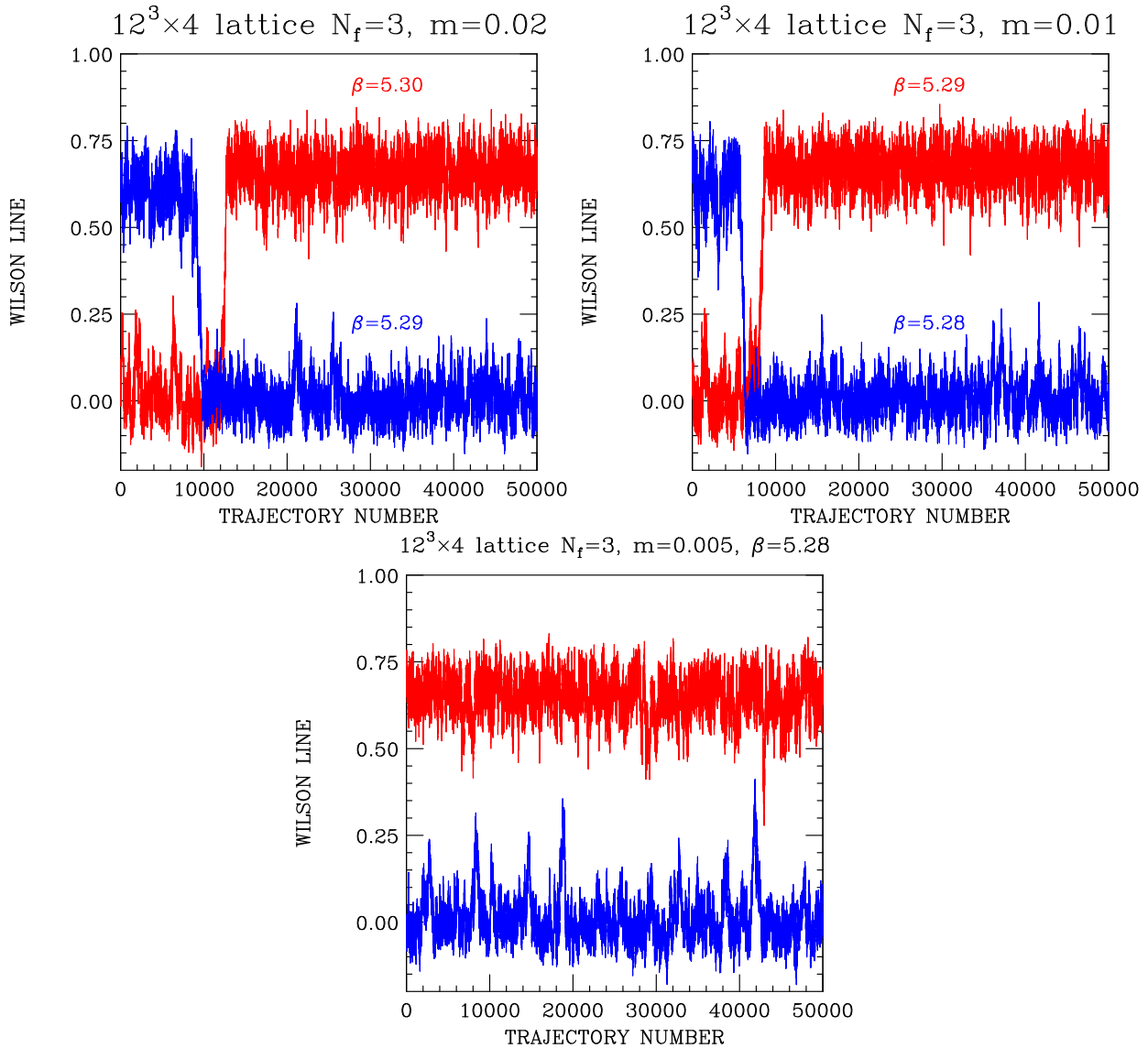


FIG. 2: a) Evolution of Wilson Line from a cold start at  $\beta = 5.3$  and from a hot start at  $\beta = 5.29$  for  $m = 0.02$ . b) Evolution of Wilson Line from a cold start at  $\beta = 5.29$  and from a hot start at  $\beta = 5.28$  for  $m = 0.01$ . c) Evolution of Wilson Line from cold and hot starts at  $\beta = 5.28$  for  $m = 0.005$ .

Now we turn to more quantitative estimates of the position of the deconfinement tran-

sitions for each of the 3 masses. We do this by examining the evolution of the Wilson Lines with molecular-dynamic ‘time’ near the transition and the observation of tunneling. Such ‘time’ histories are shown in figure 2. Part (a) of this figure shows time evolutions for  $m = 0.02$ . Starting from a cold start at  $\beta = 5.3$  we observe a tunneling from a cold (small Wilson Loop) state to a hot (large Wilson Loop) state, after which the system remains in this hot state for the rest of the run. Starting from a hot state at  $\beta = 5.29$  the system tunnels to a cold state and remains there. From this we conclude that  $\beta = 5.29$  is on the cold side of the transition and  $\beta = 5.3$  is on the hot side of the transition. Our best estimate of the position of the transition is thus  $\beta = 5.295(5)$ . Similarly from part (b) of this figure we deduce that the transition for  $m = 0.01$  lies between  $\beta = 5.28$  and  $\beta = 5.29$  giving our best estimate as  $\beta = 5.285(5)$ . Finally in part (c) we show the time evolution from hot and cold starts at  $\beta = 5.28$  for  $m = 0.005$ . Here there are no tunnelings in either case for the duration (50,000 trajectories) of each run, from which we conclude that the transition is close to  $\beta = 5.28 - \beta = 5.280(5)$ . The behaviour shown in this figure (2) strongly suggests a first-order phase transition. However, in the absence of any finite-size analysis, this observation is not conclusive.

The chiral condensate becomes small and shows a strong dependence on  $m$  for large  $\beta$ . However, naive attempts to extrapolate to zero quark mass depend strongly on the analytic form chosen for extrapolation. While we might expect a first order transition for  $N_f = 3$ , this is not obvious in the ‘data’. We therefore examine the (disconnected part of the) chiral susceptibilities discussed in section 2. These are plotted in figure 3 for all 3 quark masses.  $\chi_{\bar{\psi}\psi}$  shows a clear peak at  $\beta = 6.0$  for each quark mass. The height of the peaks increases with decreasing quark mass, as it should, since the susceptibility will diverge at the chiral phase transition. Since the  $\beta$  at the peak does not change with mass to the resolution in  $\beta$  of our simulations, we estimate that the chiral transition occurs at  $\beta = \beta_\chi = 6.0(1)$ .

We also perform a second set of simulations which start from states with the Wilson Line real and negative at  $\beta = 7.0$ . We achieve this by starting from a 2-flavour configuration with a real-negative Wilson Line also at  $\beta = 7.0$ . Again we run for 10,000 trajectories at each  $\beta$  until we get close to the transition from the state with a negative Wilson Line to a state with a complex Wilson Line with a phase close to  $\pm 2\pi/3$ , where we increase this to 50,000 trajectories. For all 3 quark masses, this transition occurs at some  $\beta$  in the range  $5.5 < \beta < 5.6$ . For  $\beta$  below 5.5 we again simulate 10,000 trajectory runs. For  $\beta \leq 5.34$  at



# $12^3 \times 4$ lattice $N_f=3$

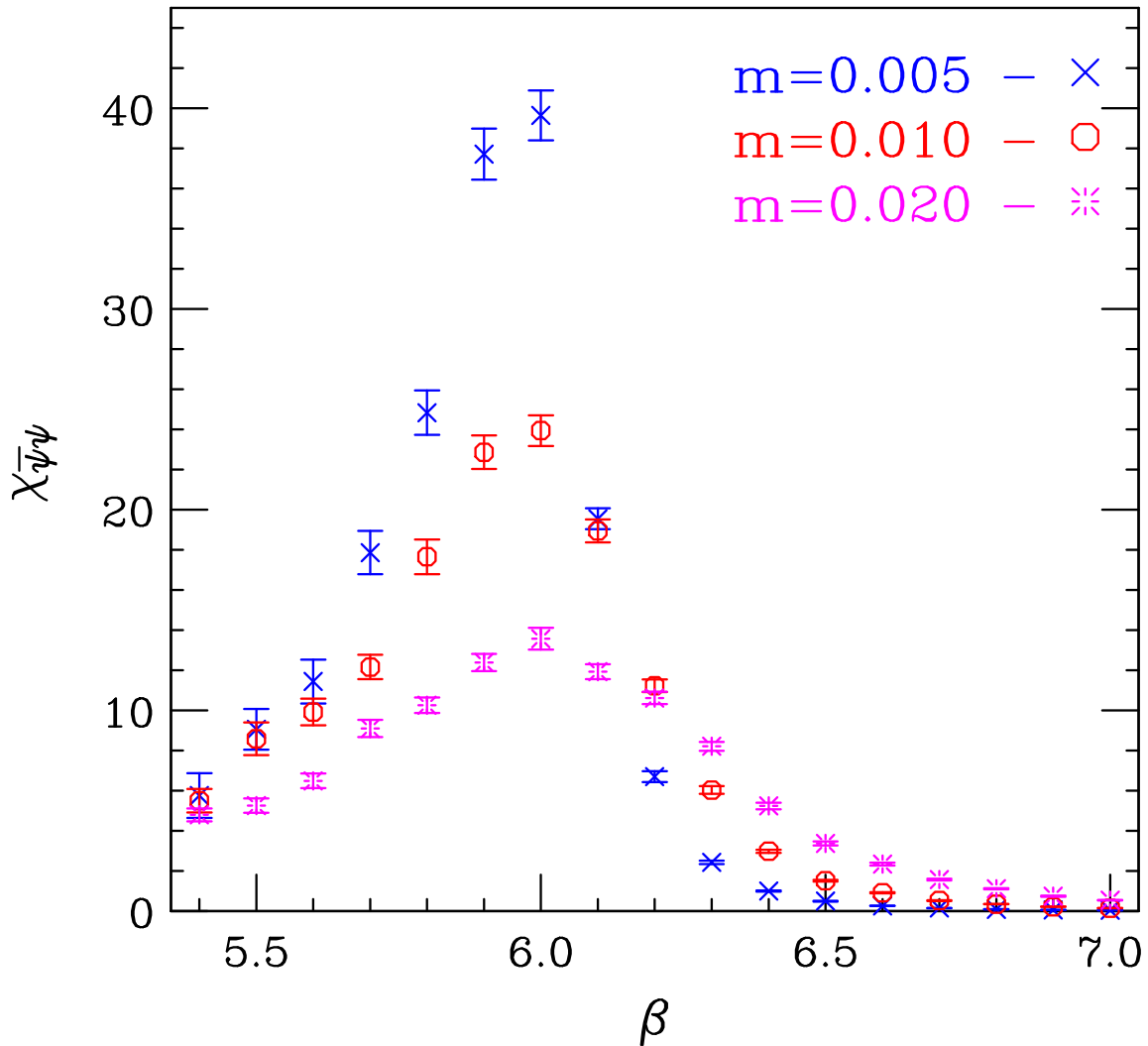


FIG. 3: Chiral susceptibilities  $\chi_{\bar{\psi}\psi}$  as functions of  $\beta$  on a  $12^3 \times 4$  lattice for  $m = 0.02, 0.01, 0.005$ , for a  $\beta$  range which includes the chiral transition.

$m = 0.02$  and  $\beta \leq 5.33$  at  $m = 0.01$  and  $m = 0.005$  we increase our run lengths to 50,000 trajectories. We perform closely spaced (in  $\beta$ ) runs down to  $\beta = 5.3$ . At  $\beta = 5.32$  and below for masses  $m = 0.02$ ,  $m = 0.01$ , and  $\beta = 5.315$  and below for  $m = 0.005$  the complex Wilson Line state rapidly decays to a positive Wilson Line state and remains there for the remainder of the run. This we take as an indication that the states with complex Wilson lines (and presumably those with negative Wilson Lines) are long-lived metastable states. We also note that just above the  $\beta$  values where this metastability reveals itself, we observe

tunnelings between the 2 complex-Wilson-Line states.

#### IV. $N_t = 6$ SIMULATIONS

We simulate lattice QCD with 3 colour-sextet quarks on  $12^3 \times 6$  lattices, starting from states with a real positive Wilson Line at  $\beta = 7.0$ , and from states with a real negative Wilson Line at  $\beta = 7.0$ . We use 3 different quark masses  $m = 0.02$ ,  $m = 0.01$  and  $m = 0.005$  to enable us to access the chiral ( $m \rightarrow 0$ ) limit. The simulations at  $\beta = 7.0$  are started from 2-flavour configurations with the same  $\beta$  and the desired Wilson Line orientation. Our runs for each  $(\beta, m)$  for each initial orientation of the Wilson Line are 10,000 trajectories in length away from the transitions, increasing to 50,000 trajectories close to the deconfinement transition, and close to the transitions from states with negative Wilson Lines to states of complex Wilson Lines. We also found it necessary to increase our statistics at  $m = 0.01$  close to the chiral transition to 25,000 trajectories to accurately determine the position of the transition. In addition, we used 20,000 trajectories for each  $(\beta, m)$  significantly below the transition, where we only have runs connected to the start with a positive Wilson line at  $\beta = 7.0$ .

As  $\beta$  is increased from its lowest value, chosen to be  $\beta = 5.3$  for each quark mass, the magnitude of the Wilson Line increases rapidly near  $\beta \approx 5.4$ , signaling the deconfinement transition. Just above this transition, there is a clear 3-state signal in the Wilson Line, where the phase of this line is close to 0 or  $\pm 2\pi/3$ . Hence we bin our ‘data’ according to which of these values the phase of the Wilson Line is closest. We are then able to combine the 2 complex-Wilson-Line bins by conjugating those Wilson Lines in the phase  $-2\pi/3$  bin. Just above the deconfinement transition we observe tunnelings between the 3 states, with no indication that any state is favoured. Hence, as far as these simulations are concerned, all 3 states appear stable (in the thermodynamic limit). In the region where this 3-state tunneling is observed, we combine the ‘data’ from the 2 starts, giving 100,000 trajectories for each  $(\beta, m)$ .

Figure 4 shows the Wilson Lines and chiral condensates  $\langle \bar{\psi}\psi \rangle$  for the state with a real positive Wilson Line, for each of the 3 masses. The rapid increase in the Wilson Line near  $\beta = 5.4$  is clear. These Wilson Line values continue to increase over the whole range of  $\beta$ s used in our simulations, and are expected to approach 3 as  $\beta \rightarrow \infty$ . The deconfinement

$12^3 \times 6$  lattice  $N_f=3$

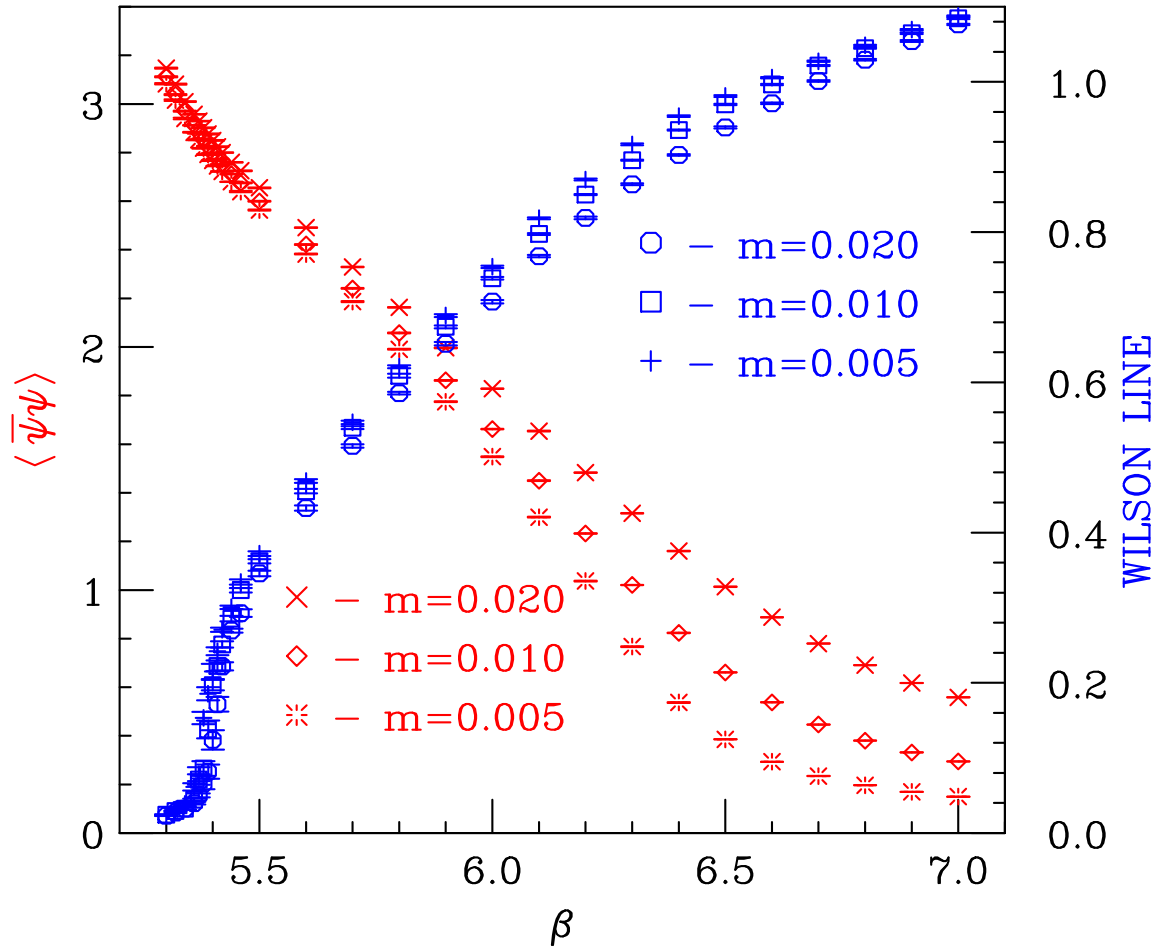


FIG. 4: Wilson Line and  $\langle \bar{\psi}\psi \rangle$  as functions of  $\beta = 6/g^2$  on a  $12^3 \times 6$  lattice, in the state with a real positive Wilson Line, for  $m = 0.02, 0.01, 0.005$ .

transition has little effect on the chiral condensates, which decrease over the range of  $\beta$ s under consideration. At larger  $\beta$  values these condensates become increasingly mass dependent, decreasing with decreasing mass, suggesting that they will vanish in the chiral limit. Just from looking at these graphs, one would suspect that the chiral transition occurs at  $\beta$  just below 6.5, but it is clear that a more reliable method, such as that provided by examining the chiral susceptibilities, is needed to determine this  $\beta_\chi$  with any precision. This qualitative analysis does indicate, however, that the deconfinement and chiral transitions are still far apart.

We now turn our attention to the states with complex or real negative Wilson Lines. First

$12^3 \times 6$  lattice  $N_f=3$

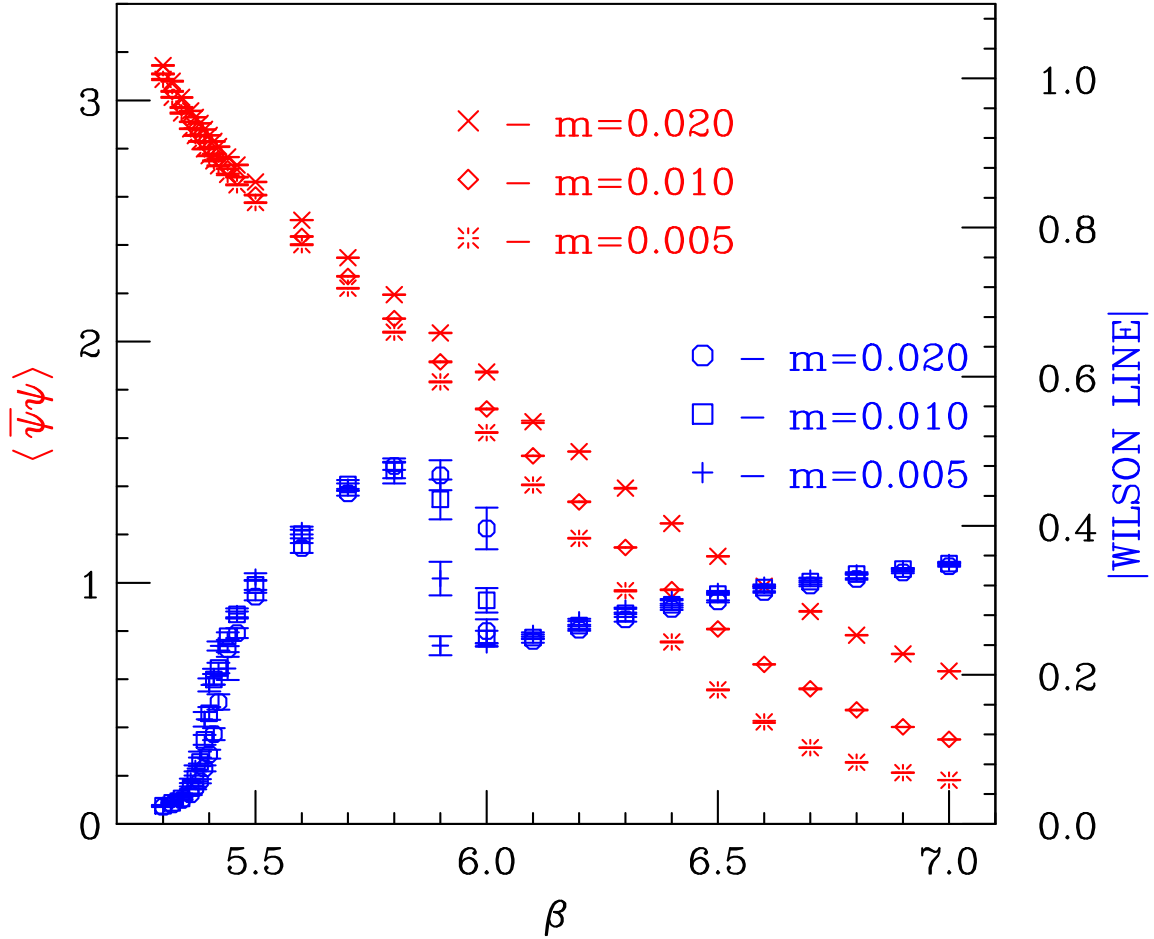


FIG. 5: Magnitude of the Wilson Line and  $\langle \bar{\psi}\psi \rangle$  as functions of  $\beta = 6/g^2$  on a  $12^3 \times 6$  lattice, in the states with complex or negative Wilson Lines, for  $m = 0.02, 0.01, 0.005$ .

we note that states having Wilson Lines with phases  $\pm 2\pi/3$  disorder to a state with a real negative Wilson Line for  $\beta$  sufficiently large. This occurs for  $5.9 \lesssim \beta \lesssim 6.0$  for  $m = 0.005$  and at slightly higher  $\beta$ s for the larger masses. In figure 5 we show the magnitudes of the Wilson Lines for states with complex or negative Wilson Lines and the corresponding chiral condensates as functions of  $\beta$  for each mass. Again the magnitude of the Wilson Line shows the deconfinement transition for  $\beta \approx 5.4$ . It also shows the transition from a complex to a real negative Wilson Line for  $\beta \approx 6$ . The chiral condensate barely responds to the deconfinement transition and shows indications that it will vanish in the chiral limit for

some  $\beta$  in the neighbourhood of the chiral transition for the positive Wilson Line state.

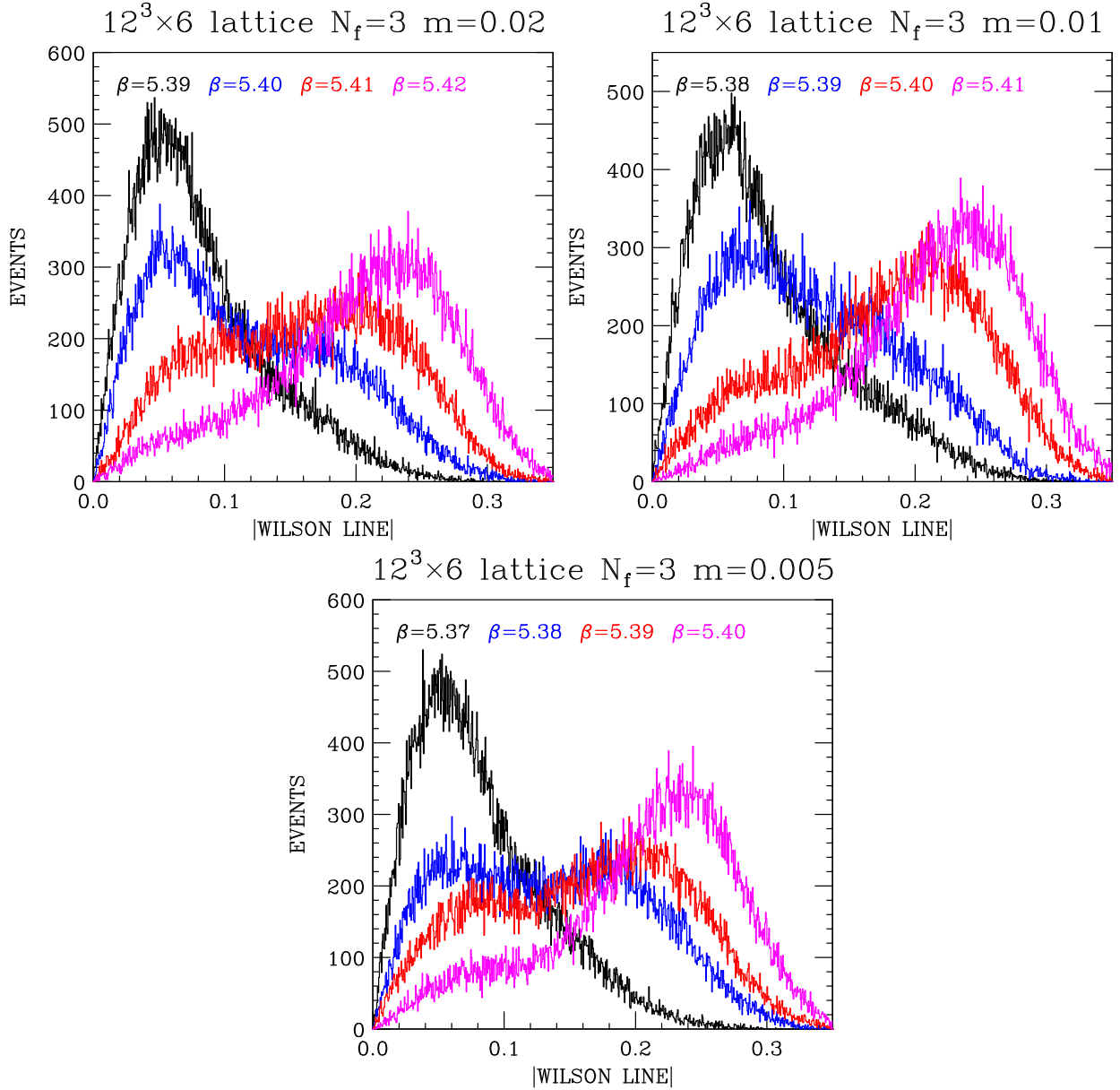


FIG. 6: Histograms of the magnitudes of Wilson Lines for  $\beta$  values bracketing the deconfinement transition on a  $12^3 \times 6$  lattice for a)  $m = 0.02$ , b)  $m = 0.01$ , c)  $m = 0.005$ .

To more accurately estimate the positions of the deconfinement transition, we histogram the magnitudes of the Wilson Lines in the vicinity of this transition. We display such histograms in figure 6. From these we estimate that our transitions occur at  $\beta = \beta_d$ , where for  $m = 0.02$   $\beta_d = 5.410(10)$ , for  $m = 0.01$   $\beta_d = 5.395(10)$  and for  $m = 0.005$   $\beta_d = 5.385(10)$ . If we assume that below  $\beta_d$  the magnitudes of the real positive and complex Wilson Lines

should be approximately the same, while above they will differ, we get estimates of  $\beta_d$  which are lower by 1–1.5 standard deviations.

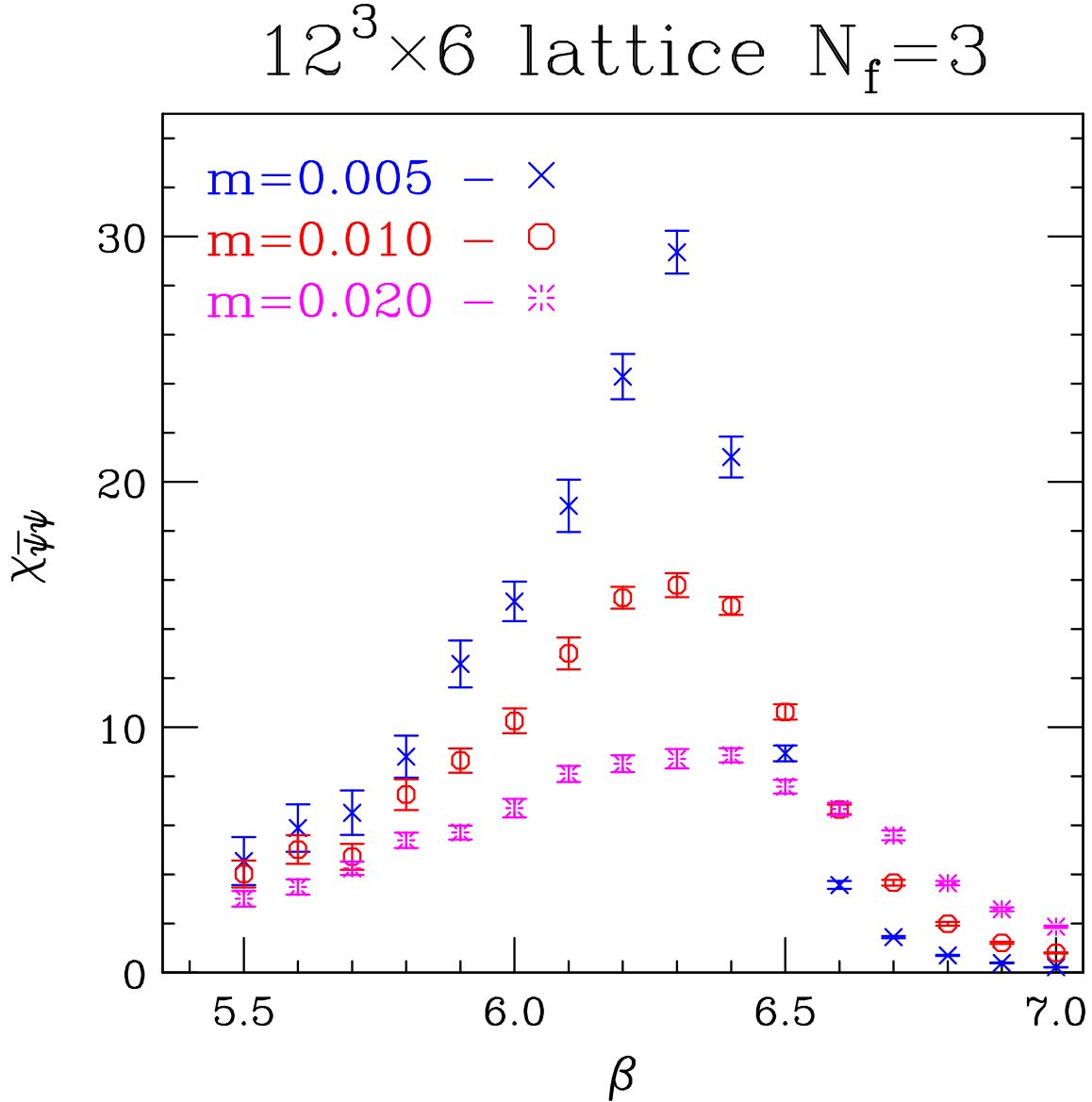


FIG. 7: Chiral susceptibilities  $\chi_{\bar{\psi}\psi}$  as functions of  $\beta$  on a  $12^3 \times 6$  lattice for  $m = 0.02, 0.01, 0.005$ , for a  $\beta$  range which includes the chiral transition.

As we have noted, determining the position of the chiral-symmetry restoration phase transition directly from the chiral condensates themselves, is difficult if not impossible, because we do not have a method of extrapolating the condensates to zero mass which we trust. Hence, to get an accurate estimate of the  $\beta$  value  $\beta_\chi$  of the chiral phase transition, we turn to a consideration of the (disconnected) chiral susceptibility  $\chi_{\bar{\psi}\psi}$ . The position

of the peak of  $\chi_{\bar{\psi}\psi}$  as a function of mass will approach  $\beta_\chi$  as  $m \rightarrow 0$ . The value of  $\chi_{\bar{\psi}\psi}$  at the peak will diverge (on a lattice of infinite spatial volume) in this limit, making the position of the peak easier to determine as the quark mass is decreased. Figure 7 shows these susceptibilities. What we observe is that the position of the peak does not move very much as  $m$  is decreased, so that the position of the peak at the lowest mass  $m = 0.005$  should give a reasonable estimate of  $\beta_\chi$ . We therefore estimate that  $\beta_\chi = 6.3(1)$ .

## V. DISCUSSION AND CONCLUSIONS

We simulate the thermodynamics of QCD with 3 flavours of colour-sextet quarks on  $12^3 \times 4$  and  $12^3 \times 6$  lattices. Table I shows our estimates for the positions of the deconfinement and chiral transitions. First we note that the chiral and deconfinement transitions are far apart as

$N_t$	$\beta_d$	$\beta_\chi$
4	5.275(10)	6.0(1)
6	5.375(10)	6.3(1)

TABLE I:  $N_f = 3$  deconfinement and chiral transitions for  $N_t = 4, 6$ . In each case we have attempted an extrapolation to the chiral limit.

was the case for 2 flavours. Both transitions move to significantly larger values of  $\beta = 6/g^2$  as  $N_t$  is increased from 4 to 6. Since we expect the 3-flavour theory to be conformal, the chiral transition should be a bulk transition occurring at fixed  $\beta$ . This suggests that we are in the strong-coupling regime where the fermions play little part in the dynamics, which is therefore quenched. We are thus seeing finite temperature transitions of the quenched theory. The move of both transitions towards weaker coupling is controlled by the asymptotic freedom of the pure gauge theory. The bulk nature of the continuum chiral transition will not reveal itself until  $N_t$  is sufficiently large for the chiral transition to emerge into the weak coupling regime. The similarity in the behaviour of the  $N_t = 4$  and 6 transitions between the 2-flavour and 3-flavour theories led us to suspect that both transitions might also lie in the strong-coupling regime for the 2-flavour theory. For 2 flavours we have since obtained results of  $N_t = 8$  simulations which, when combined with the  $N_t = 4$  and 6 results support this conclusion [10]. Thus 3-flavour simulations can help with the interpretation of the 2-flavour simulations.

The phase structure of the 3-flavour theory is also similar to the 2-flavour case. Above the deconfinement transition there is a 3-state signal, a remnant of the  $Z_3$  symmetry of the quenched theory. This is further evidence that the theory is effectively quenched at these couplings. As in the 2-flavour case, the 2 states with complex Wilson Lines disorder to a state with a real negative Wilson Line for  $\beta$  sufficiently large. For  $N_t = 4$  as for 2 flavours, only the state with a positive Wilson Line appears stable; the other states show signs of metastability. This contrasts with the  $N_t = 6$  case where all states appear stable. The existence of such states where the Wilson Line has phases  $\pm 2\pi/3$  and  $\pi$  in addition to that with phase 0 has been predicted by Machtey and Svetitsky and observed in their simulations with Wilson fermions [22].

We are now extending these simulations to  $N_t = 8$ , after which we will consider extending them to  $N_t = 12$ . This way we hope to observe the chiral transition emerge into the weak-coupling domain. If the  $N_f = 2$  theory is QCD-like, we hope that this should be adequate to distinguish the  $N_f = 2$  and  $N_f = 3$  theories.

DeGrand Shamir and Svetitsky have been studying lattice QCD with 2 colour-sextet quarks using improved Wilson quarks. The Lattice Higgs Collaboration has been studying the 2 flavour theory using improved staggered quarks. Both these collaborations have concentrated their efforts on the zero-temperature behaviour, except for some very early work.

### Acknowledgements

DKS is supported in part by the U.S. Department of Energy, Division of High Energy Physics, Contract DE-AC02-06CH11357.

This research used resources of the National Energy Research Scientific Computing Center, which is supported by the Office of Science of the U.S. Department of Energy under Contract No. DE-AC02-05CH11231. In particular, these simulations were performed on the Cray XT4, Franklin and Cray XT5, Hopper, both at NERSC. In addition this research used the Cray XT5, Kraken at NICS under XSEDE Project Number: TG-MCA99S015.



- 
- [1] S. Weinberg, Phys. Rev. D **19**, 1277 (1979).
  - [2] L. Susskind, Phys. Rev. D **20**, 2619 (1979).
  - [3] B. Holdom, Phys. Rev. D **24**, 1441 (1981).
  - [4] K. Yamawaki, M. Bando and K. i. Matumoto, Phys. Rev. Lett. **56**, 1335 (1986).
  - [5] T. Akiba and T. Yanagida, Phys. Lett. B **169**, 432 (1986).
  - [6] T. W. Appelquist, D. Karabali and L. C. R. Wijewardhana, Phys. Rev. Lett. **57**, 957 (1986).
  - [7] F. Sannino, K. Tuominen, Phys. Rev. **D71**, 051901 (2005). [hep-ph/0405209].
  - [8] D. D. Dietrich, F. Sannino, K. Tuominen, Precision measurements: Predictions for CERN LHC,” Phys. Rev. **D72**, 055001 (2005). [hep-ph/0505059].
  - [9] J. B. Kogut, D. K. Sinclair, Phys. Rev. **D81**, 114507 (2010). [arXiv:1002.2988 [hep-lat]].
  - [10] J. B. Kogut, D. K. Sinclair, [arXiv:1105.3749 [hep-lat]].
  - [11] D. K. Sinclair, J. B. Kogut, [arXiv:1111.2319 [hep-lat]].
  - [12] Y. Shamir, B. Svetitsky and T. DeGrand, Phys. Rev. D **78**, 031502 (2008) [arXiv:0803.1707 [hep-lat]].
  - [13] T. DeGrand, Y. Shamir and B. Svetitsky, Phys. Rev. D **79**, 034501 (2009) [arXiv:0812.1427 [hep-lat]].
  - [14] T. DeGrand, Phys. Rev. D **80**, 114507 (2009) [arXiv:0910.3072 [hep-lat]].
  - [15] T. DeGrand, Y. Shamir and B. Svetitsky, Phys. Rev. D **82**, 054503 (2010) [arXiv:1006.0707 [hep-lat]].
  - [16] T. DeGrand, Talk presented at Lattice2011, Squaw Valley, California (2011).
  - [17] Z. Fodor, K. Holland, J. Kuti, D. Negradi and C. Schroeder, PoS **LATTICE2008**, 058 (2008) arXiv:0809.4888 [hep-lat].
  - [18] Z. Fodor, K. Holland, J. Kuti, D. Negradi and C. Schroeder, arXiv:1103.5998 [hep-lat].
  - [19] J. Kuti, Talk presented at Lattice2011, Squaw Valley, California (2011).
  - [20] S. R. Sharpe, PoS **LAT2006**, 022 (2006) [arXiv:hep-lat/0610094].
  - [21] M. A. Clark and A. D. Kennedy, Phys. Rev. D **75**, 011502 (2007) [arXiv:hep-lat/0610047].
  - [22] O. Machtey and B. Svetitsky, Phys. Rev. D **81**, 014501 (2010) [arXiv:0911.0886 [hep-lat]].